Nucleic Acids Research, 1995, Vol. 23, No. 17 3393–3402

Conformational changes induced by DNA binding of NF-κB

James R. Matthews, John Nicholson, Ellis Jaffray, Sharon M. Kelly[1], Nicholas C. Price[1] and Ronald T. Hay*

School of Biological and Medical Sciences, Irvine Building, University of St Andrews, St Andrews, Fife KY16 9AL, UK and [1]Department of Biological and Molecular Sciences, University of Stirling, Stirling FK9 4LA, UK

Received June 4, 1995; Revised and Accepted July 21, 1995

ABSTRACT

The transcription factor NF-κB makes extensive contacts with its recognition site over one complete turn of the double helix. Structural transitions, in both protein and DNA, that accompany formation of the DNA–protein complex were analysed by proteinase sensitivity and circular dichroism (CD) spectroscopy. In the absence of DNA chymotrypsin cleaved p50 after residues Y60 and N78, while proteinase K cleaved p50 after residues S74 and Q180. Previous experiments had indicated that trypsin cleaved p50 after K77. Cleavages after Y60, S74, K77 and N78 were blocked in the presence of bound DNA, whereas cleavage after Q180 was enhanced. Y60, S74, K77 and N78 are all located in the p50 N-terminal domain AB loop, whereas Q180 is located in the mainly α-helical region between p50 N-terminal domain β-strands G′ and H. As only Y60 makes direct contact with the DNA it is likely that the AB loop is highly unstructured in the absence of DNA, but is held in a rigid, proteinase-resistant structure by bound DNA. These conclusions were supported by CD spectroscopic studies of recombinant p50 and p65 homodimers, which indicated that both species changed conformation when binding DNA. Examination of the near UV CD spectra revealed that with some DNA sequences the bound and free forms of the DNA assumed different conformations. While this was evident for a fully symmetrical, high affinity recognition site DNA, it was not apparent with less tightly bound DNA.

INTRODUCTION

The NF-κB/rel/dorsal family of dimeric transcription factors have been implicated in the transcriptional control of the expression of a variety of eukaryotic cellular and viral genes (reviewed in 1). Members of this family include the p50 (NF-κB1) (2,3), p52 (NF-κB2) (4,5), p65 (Rel A) (6,7), Rel B (8,9), c-Rel (10), v-Rel (11), dorsal (12) and Dif (13) proteins. These family members all possess a highly conserved region of ~300 amino acids (termed the NRD region) in their N-termini which is responsible for the dimerization, DNA binding and nuclear localization functions of these proteins (reviewed in 14). Although the prototypical form of NF-κB is a p50–p65 heterodimer (15), NF-κB family members can form homo- and heterodimers to generate species with subtly differing affinities for DNA sequences related to the κB motif (5′-GGGACTTTCC-3′), first identified in the immunoglobulin κ light chain gene major intron transcriptional enhancer (16).

Several studies of NF-κB family members have identified the importance of amino acid residues in the N-terminal part of the NRD region in determining DNA binding specificity. For example, a fusion protein containing residues 35–68 of human p50 with residues 46–309 of human p65 showed p50-type DNA binding specificity. Further, a single amino acid change (H67R) in the p50 sequence conferred p65-type DNA binding specificity on the fusion protein (17). Other groups have similarly demonstrated that mutation of the p50 C62 residue resulted in altered DNA binding specificity (18) and that single amino acid changes affecting DNA binding were clustered between residues 54 and 70 of human p50 (19). More recently, photocrosslinking studies using the β-interferon gene type κB site yielded crosslinks to p50 residues Y60 and H67 (20). The conserved p50 C62 residue was shown to be in close contact with κB motif DNA (18), thus explaining the importance of this residue in the redox modulation of NF-κB protein DNA binding activity (19,21–24).

Studies using proteinases as probes of NF-κB structure have indicated that binding of p50 homodimers to high affinity types of κB motif, such as that found in the MHC Class I $H2K^b$ gene (5′-GGGGATTCCCC-3′), gives almost complete protection of p50 against cleavage by trypsin on the C-terminal side of the K77 residue. It was suggested that bound DNA might mask this trypsin cleavage site or, more interestingly, might induce a conformational change in the p50 structure, as in the absence of DNA the entire p50 protein was degraded (25). Other workers have similarly shown that the sensitivity of p50–DNA complexes towards cleavage by chymotrypsin depended on the precise sequence of the bound DNA. Although the site(s) of chymotrypsin cleavage were not determined, it was suggested that a conformational change occurred in p50 upon binding to the $H2K^b$ type of κB site (26).

The recent X-ray crystallographic structure determinations of p50 homodimer–DNA co-crystals (27,28) have now made it possible to confirm many of the above proposals. These studies indicated that the p50 polypeptide chain comprises two domains

* To whom correspondence should be addressed

which are organized into antiparallel β-barrels. Both N- and C-terminal domains contribute a number of flexible loops to the formation of a large DNA binding surface which fills the entire major groove of the bound DNA. The p50 homodimer interface being formed by side chains from three β-strands in the C-terminal domain interacting symmetrically with the corresponding residues in the opposing subunit. The p50 N- and C-terminal domains are connected by a potentially flexible 10 residue linker and are flanked by polypeptide regions whose structures were too disordered to appear in the electron density map.

The overall architecture of the p50 N-terminal domain is of a nine-stranded antiparallel β-barrel, with several of the intervening loops in the polypeptide chain being critical for DNA binding activity. The only region of α-helical structure in the DNA–protein complex lies in the large loop between the N-terminal domain G′ and H β-strands (adopting the nomenclature used in 27), much of this region being unique to p50 among NF-κB family members. The architecture of the p50 C-terminal domain consists of seven antiparallel β-strands, again arranged with a β-sandwich core folding pattern, with intervening loops in the polypeptide chain again having an important role in stabilizing the DNA–protein complex (27,28).

Many of the specific base and backbone contacts with κB motif DNA are contributed by part of the AB loop(s) connecting the A and B β-strands of the p50 N-terminal domain(s), with p50 residues between amino acids 57 and 67 making base contacts in the major groove and contacting phosphates in the backbone of the DNA. The overall AB loop comprises residues 50–82 in the human p50 sequence (27) and has an extended structure in the κB motif DNA–p50 protein co-crystal. The use of an AB loop from each monomer to recognize a single half site in κB motifs explains the results of earlier methylation protection and alkylation interference studies and of hydroxyl radical footprinting studies. These demonstrated that NF-κB makes base and backbone contacts with the κB motif over one complete turn of the DNA double helix and suggested that NF-κB made its sequence-specific contacts via the major groove of the DNA (29–31). This type of arrangement also explains the discrete half-site DNA binding specificities seen with NF-κB family heterodimers (32,33).

In its DNA-bound form p50 appears like a clamp that fits into the major groove, almost encircling the DNA. To disengage from the DNA the 'jaws' of the clamp must open and likewise must close when the DNA is bound. The protein must therefore display a considerable degree of conformational flexibility. To investigate these changes in protein conformation we have employed proteinase accessibility and circular dichroism (CD) spectroscopy. In the absence of DNA the AB loop is susceptible to proteolytic cleavage, but when DNA is bound these cleavages are blocked, even in regions which may not be in direct contact with DNA. In contrast, cleavage in a mainly α-helical region between the p50 N-terminal domain β-strands G′ and H was enhanced in complexes with the high affinity H2TF1 type of κB motif. CD spectroscopy revealed that binding of specific or non-specific DNA to either p50 or p65 homodimers resulted in conformational changes in the NF-κB proteins. In contrast, changes in the conformation of the DNA in complexes with p50 or p65 homodimers were restricted to those oligonucleotides bearing high affinity κB motifs. These results indicate that conformational changes occur in both the NF-κB protein and in the κB motif DNA upon formation of the specific DNA–protein complex.

MATERIALS AND METHODS

Bacterial expression and purification of NF-κB proteins

NF-κB p50 protein comprising residues 35–381 was expressed as a glutathione S-transferase fusion protein in *Escherichia coli* JM101 and the fusion protein purified using a glutathione–Sepharose affinity column as described previously (23). The GST–p50 fusion protein was eluted from the affinity column in 50 mM Tris–HCl, pH 7.0, 0.5 M NaCl, 10 mM reduced glutathione before cleavage with thrombin (1 U/mg protein). The thrombin digestion was terminated by the addition of PMSF to 1 mM and the NaCl concentration reduced to 0.25 M by dilution prior to loading onto a double-stranded calf thymus DNA–Sepharose column previously equilibrated with 20 mM sodium phosphate buffer, pH 7.0, 0.2 M NaCl, 2 mM DTT. After washing the bound p50 protein was eluted with 20 mM sodium phosphate, pH 7.0, 0.6 M NaCl. Peak protein fractions were frozen in liquid nitrogen and stored at –70°C. The NF-κB p65 protein construct (corresponding to amino acid residues 12–317, from a cDNA clone supplied by Dr C. Rosen) was expressed and purified in a similar way. The purity of the p50 and p65 proteins was determined by SDS–PAGE on 10% polyacrylamide gels under reducing conditions.

Proteolytic digestion of NF-κB proteins

Digestions of recombinant p50 homodimers with chymotrypsin were carried out in 20 μl aliquots containing 43 μg p50 (27.9 μM p50 homodimer) in 20 mM sodium phosphate, pH 7.0, 0.5 M NaCl and either no chymotrypsin or chymotrypsin at substrate:enzyme ratios (w/w) of 10.8:1, 21.5:1, 43:1, 86:1, 172:1, 344:1, 689:1, 1380:1, 2760:1 and 5510:1. Similarly, digestions of recombinant p50 with proteinase K were carried out in 20 μl containing 43 μg p50 in 20 mM sodium phosphate, pH 7.0, 0.5 M NaCl and either no proteinase K or proteinase K at substrate:enzyme ratios (w/w) of 43:1, 86:1, 172:1, 344:1, 689:1, 1380:1, 2760:1, 5510:1, 11 000:1 and 22 000:1. After incubation for 1 h at 20°C proteinases were inactivated by addition of PMSF to 1 mM and the digestion products stored at –20°C. Digestion of p50 homodimers in the presence or absence of κB motif oligonucleotides was carried out in a volume of 27 μl containing 10 μg recombinant p50 (4.81 μM p50 homodimer) with a 6.5-fold molar excess (31.3 μM) of HIV-L or H2TF1 κB motif double-stranded oligonucleotide and the appropriate dilution of chymotrypsin or proteinase K in 20 mM sodium phosphate, pH 7.0, to give a total NaCl concentration of 200 mM. The digestions were carried out with p50 substrate:chymotrypsin ratios (w/w) of 3.12:1, 6.25:1, 12.5:1, 25:1, 50:1, 100:1, 200:1 and 400:1 or with p50 substrate:proteinase K ratios (w/w) of 12.5:1, 25:1, 50:1, 100:1, 200:1, 400:1, 800:1 and 1600:1. Reactions were incubated for 1 h at 20°C, proteinases inactivated by the addition of PMSF to 1 mM and digestion products analysed by SDS–PAGE.

SDS–PAGE and Western blotting

Digestion products of p50 homodimers with chymotrypsin and proteinase K were analysed by electrophoresis in the presence of SDS in reducing 10% polyacrylamide gels (with 29:1 acrylamide:bisacrylamide) according to Laemmli (34). Following gel electrophoresis proteins were either stained directly using

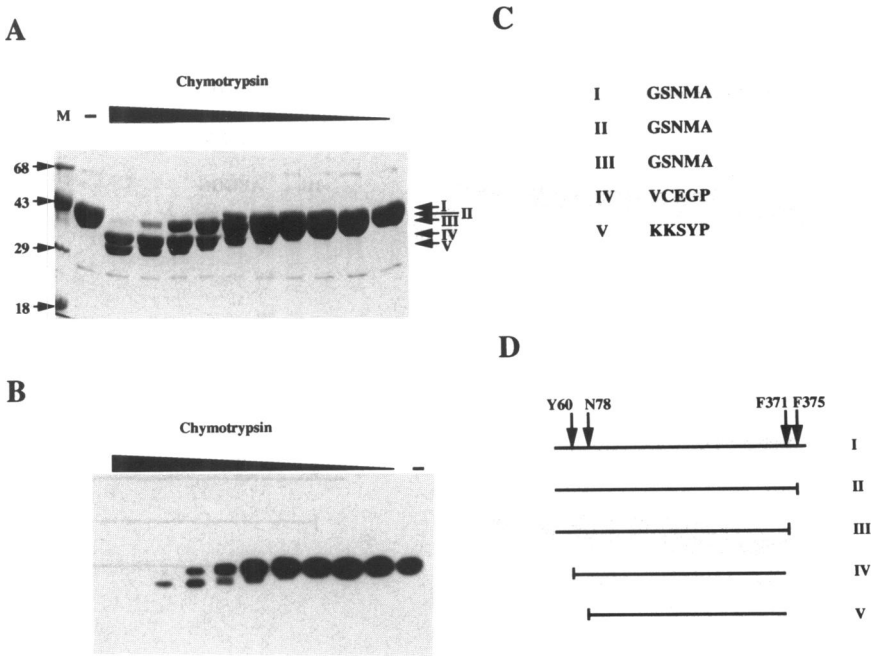

Figure 1. Chymotrypsin cleavage of p50 homodimers. (**A**) p50 (27.9 μM homodimer) was digested with chymotrypsin at substrate:protease ratios of 10.8:1, 21.5:1, 43:1, 86:1, 172:1, 344:1, 689:1, 1380:1, 2760:1, and 5510:1. Digestion products (21.5 μg p50) were resolved in a 10% polyacrylamide gel containing SDS and stained with Coomassie blue. The masses of the molecular weight standards (M) are indicated in kDa. (**B**) The same digestion products (0.14 μg p50) were also analysed by Western blotting with monoclonal antibody 3B6, which recognises the nuclear localization signal of p50 (amino acids 362–366). (**C**) Digestion products were electrophoretically transferred to Problot and the N-terminal amino acid sequence of fragments I–IV determined. (**D**) Deduced structure of the chymotrypsin digestion products. The indicated amino acids are N-terminal to the cleavage site.

Coomassie brilliant blue or the SDS–protein complexes were electroblotted onto polyvinylidene difluoride (PVDF; Sigma) membrane using an LKB semi-dry blotter with a 20 mM Tris, 150 mM glycine, 20% methanol transfer buffer. PVDF membranes were blocked for 1 h in phosphate-buffered saline (PBS), 0.1% Tween-20, 10% non-fat dry milk (PTM) before incubation for 1 h at 20°C with monoclonal antibody 3B6 tissue culture supernatant (35) diluted 1:10 with PTM. PVDF membranes were washed twice with PTM prior to incubation for 30 min at 20°C with horseradish peroxidase-conjugated sheep anti-mouse immunoglobulin (Amersham; diluted 1:3000 in PTM). Membranes were washed twice with PTM and twice with PBS, 0.1% Tween-20 before images were developed in enhanced chemiluminescence detection reagent (Amersham) and exposed to X-ray film.

Protein sequencing

For N-terminal sequencing of p50 proteolytic fragments SDS–PAGE on a pre-run 10% polyacrylamide gel (37.5:1 acrylamide:piperazine diacrylamide ratio) used an electrophoresis anode buffer supplemented with 50 mM sodium thioglycolate. After SDS–PAGE was complete protein fragments were electroblotted onto sequencing membrane (Pro-Blott; Applied Biosystems) using a wet blotter (Mini Protean Trans-Blot cell; BioRad) with a 10 mM CAPS, 10% methanol, pH 11.0, blotting buffer. After transfer the membrane was briefly stained with amido black, then destained with frequent changes of ultrapure water. Protein bands were excised and stored at –20°C prior to N-terminal sequencing (Procise 491; Applied Biosystems).

Circular dichroism spectroscopy

To allow CD spectra to be measured in the near (320–240 nm) and far (260–200 nm) ultraviolet (UV) regions both p50 and p65 NF-κB proteins were dialysed overnight with several intermediate stages from 20 mM sodium phosphate, pH 7.0, 0.6 M NaCl into a 10 mM sodium phosphate, pH 7.5, 50 mM NaF, 0.5 mM DTT buffer to yield a buffer with a relatively low UV absorbance. Similarly, the double-stranded specific and non-specific DNA oligonucleotides were prepared in 10 mM sodium phosphate, pH 7.5, 50 mM NaF buffer. CD spectra were recorded using a Jasco J-600 spectropolarimeter. For each experiment dialysis buffer blank, protein only, oligonucleotide only and 1:1 molar ratio of NF-κB homodimer:double-stranded oligonucleotide spectra allowed the detection of any changes in the CD spectrum of either NF-κB protein or oligonucleotide in the protein–DNA complex.

The following oligonucleotides were used for specific and non-specific binding site DNA in the proteolysis and CD studies: H2TF1, 5′-GATCTGGGGATTCCCCAG-3′; HIV-L, 5′-GATCTAGGGACTTTCCGCG-3′; NFIII, 5′-GATCCTCACGCCTTATTTGCATATTAACTCA-3′; with their respective complementary strands generating single-stranded 5′-GATC overhangs at either end of the duplexes.

RESULTS

Chymotrypsin and proteinase K digestion of p50 in the absence of DNA

Previous studies had demonstrated that the DNA binding activity of p50 homodimers could be abolished by limited digestion with

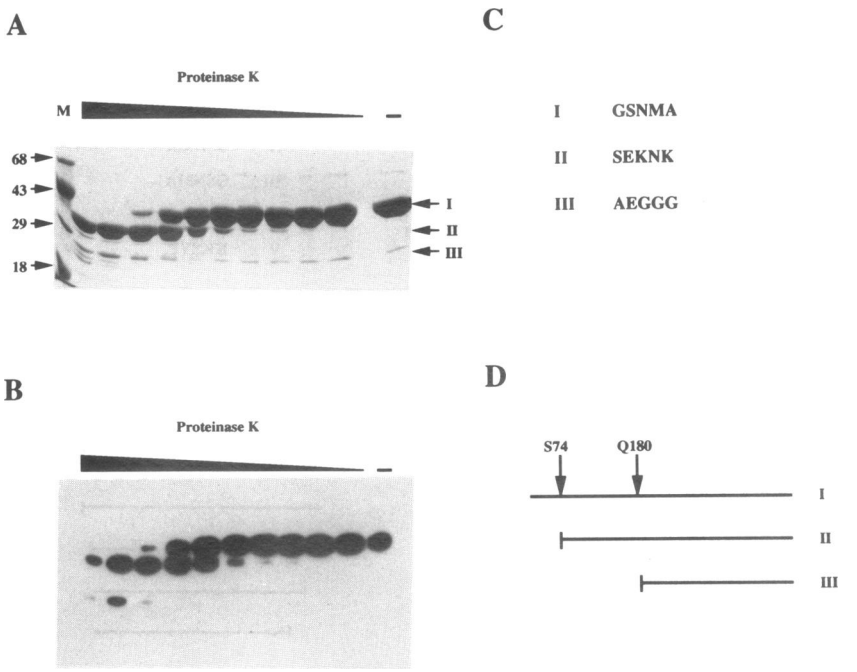

Figure 2. Proteinase K cleavage of p50 homodimers. (**A**) p50 (27.9 μM homodimer) was digested with proteinase K at substrate:protease ratios of 43:1, 86:1, 172:1, 344:1, 689:1, 1380:1, 2760:1, 5510:1, 11 000:1 and 22 000:1. Digestion products (21.5 μg p50) were resolved in a 10% polyacrylamide gel containing SDS and stained with Coomassie blue. The masses of the molecular weight standards (M) are indicated in kDa. (**B**) The same digestion products (0.14 μg p50) were also analysed by Western blotting with monoclonal antibody 3B6, which recognizes the nuclear localization signal of p50 (amino acids 362–366). (**C**) Digestion products were electrophoretically transferred to Problot and the N-terminal amino acid sequence of fragments I–III determined. (**D**) Deduced structure of the proteinase K digest products. The indicated amino acids are N-terminal to the cleavage site.

trypsin, chymotrypsin or proteinase K (25,26; J. R. Matthews, unpublished observations). To characterize sites cleaved by chymotrypsin p50 was incubated with increasing concentrations of chymotrypsin and the products of digestion analysed by SDS–PAGE. Gels were either stained directly with Coomassie brilliant blue (Fig. 1A) or analysed by Western blotting with the 3B6 monoclonal antibody (Fig. 1B), which has an epitope including the p50 nuclear localization signal (35).

As the 3B6 MAb epitope is located very close to residues 362–366 of the recombinant p50 (amino acids 35–381), Western blot reactivity of proteolytic fragments with the 3B6 MAb is a good indicator of those p50 fragments having C-termini which are intact, at least up to the nuclear localization signal region. It has already been shown that cleavage of p50 by trypsin at the C-terminal side of residue R362 does not affect the p50 DNA binding activity (35).

Comparison of Figure 1A and B shows that an early chymotrypsin cleavage occurs to generate forms of p50 which can still be recognized by the 3B6 MAb. A combination of N-terminal sequencing and mass spectroscopic analysis indicated that these forms (forms II and III) represent cleavage at the C-terminal side of residues F375 and F371 respectively (Fig. 1C and D). As the chymotrypsin concentration increases the p50-derived form III species is digested further to yield a species (form IV) of 34 kDa mass which no longer reacts with the 3B6 MAb. N-terminal amino acid sequencing of this form IV species revealed that it derived from p50 cleavage at the C-terminal side of residue Y60 (Fig. 1C and D). At still higher ratios of chymotrypsin to p50 a fragment of 32 kDa mass begins to appear (form V). N-terminal amino acid sequencing of the form V species indicated that it derived from p50 cleavage by chymotrypsin at the C-terminal side of residue N78 (Fig. 1C and D).

In the proteinase K digestions the initial p50 cleavage product (form II) has a mass of 34 kDa (Fig. 2A) and is fairly resistant towards further digestion, although it is gradually digested to yield a species of ~26 kDa mass (form III) at high proteinase K concentrations. Both the 34 kDa (form II) and 26 kDa (form III) p50-derived species react with the 3B6 MAb on a Western blot (Fig. 2B) and hence have essentially intact C-termini. N-terminal amino acid sequencing revealed that form II derived from cleavage of p50 by proteinase K at the C-terminal side of residue S74, while form III had been cleaved by proteinase K at the C-terminal side of residue Q180 (Fig. 2C and D).

N-terminal amino acid sequencing of very lightly proteinase K-digested p50 has also indicated that a very early proteinase K cleavage event occurs at the C-terminal side of p50 residue T39 (data not shown), however, these extreme N-terminal residues of p50 do not contribute to the NRD region.

Chymotrypsin and proteinase K digestion of p50 in the presence of κB motif DNA

When the proteolytic digestions of NF-κB p50 with chymotrypsin and proteinase K were repeated in the presence of the HIV-L and the high affinity MHC class I $H2K^b$ (H2TF1) type κB motifs dramatic changes in the digestion pattern were apparent. Digestion of p50 with chymotrypsin in the absence of DNA showed the same pattern of digest products as before, with the initial p50

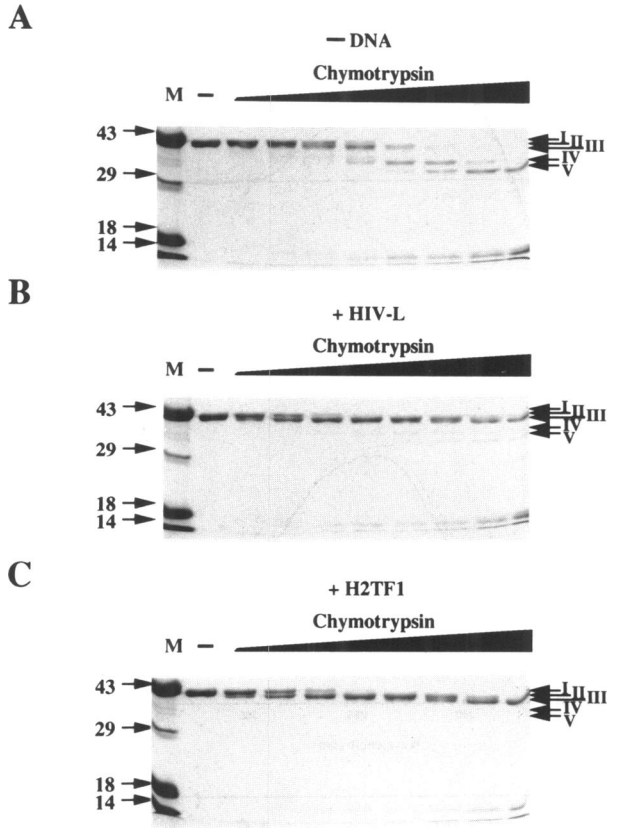

Figure 3. Chymotrypsin cleavage of p50 in the presence and absence of bound DNA. p50 (4.8 μM homodimer), either in the absence or presence DNA, was digested with chymotrypsin at substrate:protease ratios (w/w) of 400:1, 200:1, 100:1, 50:1, 25:1, 12.5:1, 6.25:1 and 3.12:1. Digestion products (5 μg p50) were resolved in 10% polyacrylamide gels containing SDS and stained with Coomassie blue. The masses of the molecular weight standards (M) are indicated in kDa. (**A**) Digestion in the absence of DNA. (**B**) Digestion in the presence of HIV-L κB motif DNA (6.5-fold molar excess with respect to p50 homodimer). (**C**) Digestion in the presence of H2TF1 κB motif DNA over p50 homodimer (6.5-fold molar excess with respect to p50 homodimer).

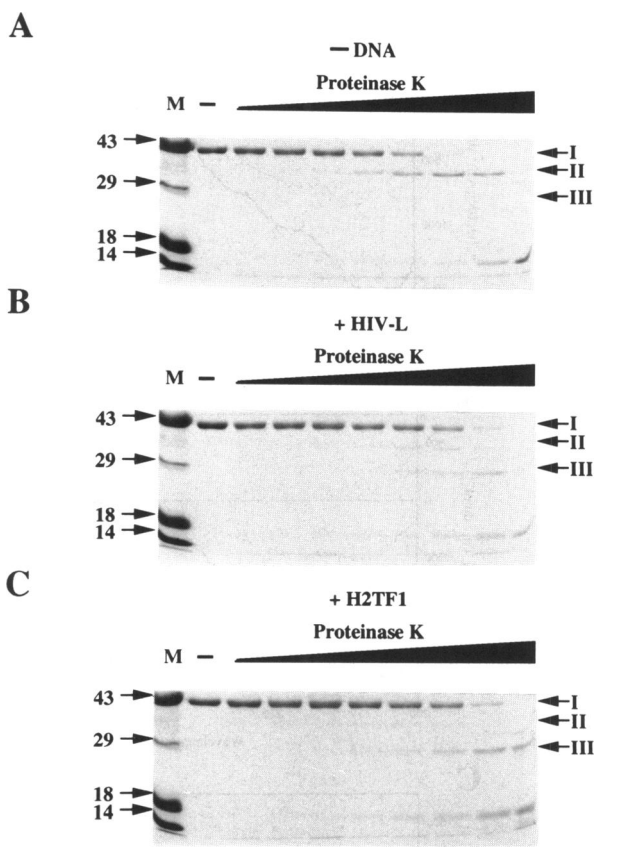

Figure 4. Proteinase K cleavage of p50 in the presence and absence of bound DNA. p50 (4.8 μM homodimer), either in the absence or presence DNA, was digested with proteinase K at substrate:protease ratios (w/w) of 1600:1, 800:1, 400:1, 200:1, 100:1, 50:1, 25:1 and 12.5:1. Digestion products (5 μg p50) were resolved in 10% polyacrylamide gels containing SDS and stained with Coomassie blue. The masses of the molecular weight standards (M) are indicated in kDa. (**A**) Digestion in the absence of DNA. (**B**) Digestion in the presence of HIV-L κB motif DNA (6.5-fold molar excess with respect to p50 homodimer). (**C**) Digestion in the presence of H2TF1 κB motif DNA over p50 homodimer (6.5-fold molar excess with respect to p50 homodimer).

cleavages at the C-terminal side of residues F375 and F371 (forms II and III). At higher concentrations of chymotrypsin relative to p50 the 34 kDa species, which has been cleaved at the C-terminal side of residue Y60 (form IV), begins to predominate, followed by the 32 kDa species cleaved at the C-terminal side of residue N78 (form V) at still higher chymotrypsin concentrations (Fig. 3A). In the presence of the HIV-L/immunoglobulin type κB motif oligonucleotide p50 is much more resistant towards cleavage at residues Y60 and N78, although cleavage still occurs at residues F375 and F371 to generate forms II and III (Fig. 3B). In contrast, in the presence of the higher affinity $H2K^b$ (H2TF1) type of κB motif chymotrypsin cleaves only at the C-terminal residues F375 (form II) and F371 (form III), with no evidence of cleavage at the N-terminal residues Y60 and N78 (Fig. 3C).

As expected, digestion of p50 with proteinase K in the absence of DNA yields the 34 kDa (form II) species, generated by cleavage at the C-terminal side of residue S74, and the minor 26 kDa (form III) species, cleaved at the C-terminal side of residue Q180 (Fig. 4A). The 32 kDa species detected between the p50 digest forms II and III is proteinase K, as shown by its N-terminal amino acid sequence and its mass. In the presence of the HIV-L κB motif oligonucleotide the p50 homodimer is much more resistant towards digestion by proteinase K at residue S74, to generate the 34 kDa (form II) species, while the amount of the form III product cleaved at p50 residue Q180 is increased (Fig. 4B). When complexed with the H2TF1 κB motif oligonucleotide the NF-κB p50 homodimer is still more resistant towards cleavage by proteinase K at residue S74, to generate the 34 kDa (form II) species. In contrast, the amount of the p50 form III product cleaved at residue Q180 is further increased in the presence of the bound H2TF1 κB motif oligonucleotide (Fig. 4C).

Thus the formation of complexes between p50 homodimers and κB motif oligonucleotides yields different proteolytic sensitivities depending on the exact nature of the κB motif, as suggested by Fujita and co-workers (26). The present study identifies the NF-κB p50 N-terminal domain AB loop and the (mainly α-helical) region between p50 N-terminal domain β-strands G′ and H as regions whose conformations are altered when p50 homodimers bind DNA.

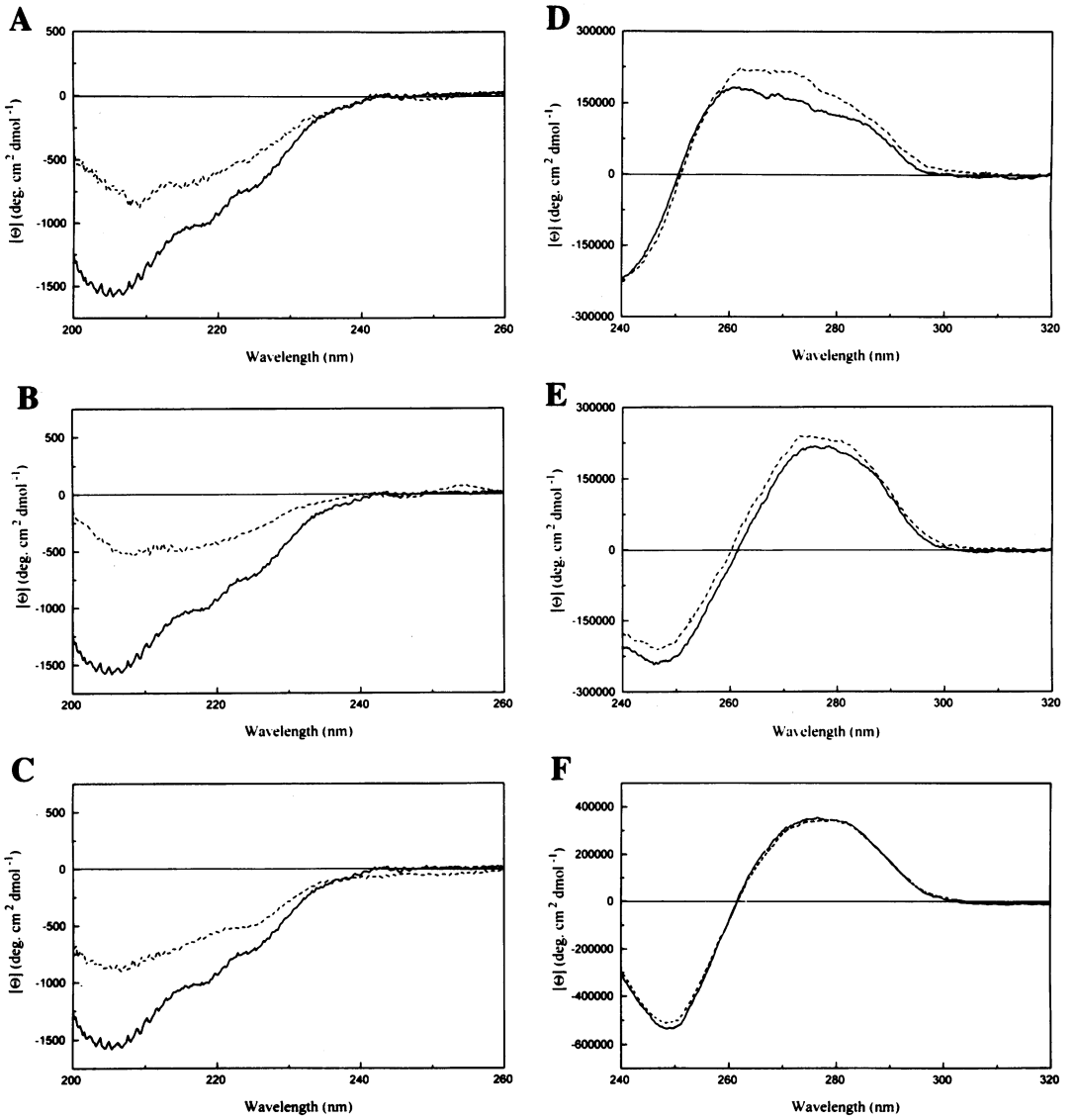

Figure 5. Circular dichroism spectroscopy of p50 binding to DNA. (**A**) Far UV CD spectrum of 9.5 μM p50 homodimers ± 9.5 μM double-stranded H2TF1 oligonucleotide (1:1 molar ratio). (**B**) Far UV CD spectrum of 9.5 μM p50 homodimers ± 9.5 μM double-stranded HIV-L oligonucleotide (1:1 molar ratio). (**C**) Far UV CD spectrum of 9.3 μM p50 homodimers ± 15.6 μM double-stranded non-specific NFIII oligonucleotide (1:1.7 molar ratio). (**D**) Near UV CD spectrum of 6.3 μM p50 homodimers ± 6.3 μM double-stranded H2TF1 oligonucleotide (1:1 molar ratio). (**E**) Near UV CD spectrum of 6.3 μM p50 homodimers ± 6.3 μM double-stranded HIV-L oligonucleotide (1:1 molar ratio). (**F**) Near UV CD spectrum of 6.3 μM p50 homodimers ± 6.3 μM double-stranded non-specific NFIII oligonucleotide (1:1 molar ratio). In (A)–(C) the ellipticity values are given in terms of the mean residue weight of p50. The solid lines represent the protein alone and the dashed lines represent the protein plus oligonucleotide, after correction for the contribution of the oligonucleotide. In (D)–(F) the ellipticity values are given in terms of the molar concentration of oligonucleotide. The solid lines represent the oligonucleotide alone and the dashed lines represent the oligonucleotide plus protein, after correction for the contribution of the protein.

Circular dichroism studies of conformational changes in NF-κB–DNA complexes

CD spectroscopy was performed with the recombinant p50 homodimer and p65 homodimer NF-κB proteins either alone or in the presence of various DNA sequences which are bound either weakly and non-specifically or tightly and with a high degree of specificity. DNA sequences selected for study were the high affinity H2TF1 type of κB motif, the HIV-L/immunoglobulin type of κB motif and non-specific nuclear factor III (NFIII) double-stranded binding site oligonucleotides. At the concentration of DNA and protein dimer (10^{-5} M) used in the analysis the equilibrium of the reaction will be such that in each case the DNA–protein complex will be the predominant form present. The far UV CD spectra of p50 homodimer in the absence and presence of specific and non-specific binding site DNA are shown in Figure 5A–C. It is clear that binding of DNA is accompanied by modification of the p50 CD spectrum that can be interpreted as changes in the secondary structure content of the protein. Application of the CONTIN procedure (36) to the spectrum over the range 200–240 nm recorded in the absence of DNA indicated that the predominant secondary structure was β-sheet, with little or no α-helix (0% α-helix, 53% β-sheet, 47% remainder). On addition of either specific or non-specific DNA the CONTIN

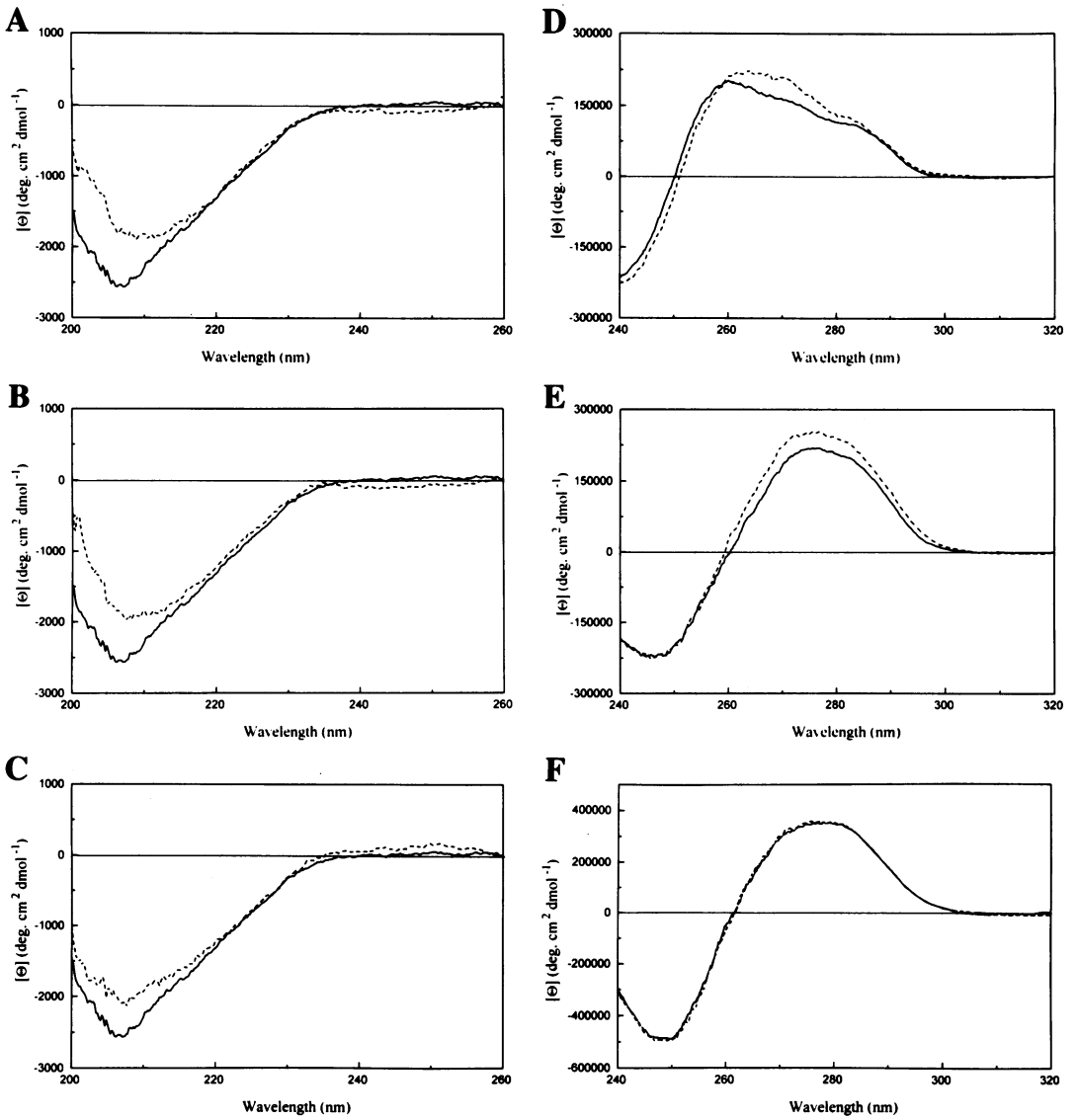

Figure 6. Circular dichroism spectroscopy of p65 binding to DNA. (**A**) Far UV CD spectrum of 21 μM p65 homodimers ± 21 μM double-stranded H2TF1 oligonucleotide (1:1 molar ratio). (**B**) Far UV CD spectrum of 21 μM p65 homodimers ± 21 μM double-stranded HIV-L oligonucleotide (1:1 molar ratio). (**C**) Far UV CD spectrum of 21 μM p65 homodimers ± 35 μM double-stranded non-specific NFIII oligonucleotide (1:1.7 molar ratio). (**D**) Near UV CD spectrum of 16 μM p65 homodimers ± 16 μM double-stranded H2TF1 oligonucleotide (1:1 molar ratio). (**E**) Near UV CD spectrum of 16 μM p65 homodimers ± 16 μM double-stranded HIV-L oligonucleotide (1:1 molar ratio). (**F**) Near UV CD spectrum of 16 μM p65 homodimers ± 16 μM double-stranded non-specific NFIII oligonucleotide (1:1 molar ratio). For the significance of the lines and the scales of ellipticity values refer to the legend to Figure 5.

procedure indicated that a small decrease in β-sheet had occurred (to 49% in the case of the H2TF1 oligonucleotide), with a corresponding increase in the remainder content. The X-ray data on the p50 homodimer–DNA co-crystal complex (27,28) indicate β-sheet and α-helix contents of ~35 and 9% respectively, values which show reasonable agreement with the predictions from the CONTIN analysis of the p50 homodimer far UV CD spectrum. Although the CD spectra indicate that binding of DNA leads to a conformational change in the protein, it is not possible to define the precise secondary structure changes that are taking place.

Examination of the near UV CD spectra reveals distinct differences in the behaviour of the three oligonucleotide species upon formation of protein–DNA complexes. The near UV CD spectrum of the high affinity H2TF1 type of κB motif is asymmetric and unlike that of typical B-form DNA. Upon formation of the high affinity specific protein–DNA complex the molar ellipticity increases, which is consistent with an increase in the degree of base stacking in the H2TF1 duplex upon complex formation. Further, both the wavelength of the maximum and the shape of the H2TF1 κB motif CD spectrum change, indicative of conformational changes being induced in the H2TF1 oligonucleotide (Fig. 5D). The near UV CD spectrum of the HIV-L type of κB motif is, in contrast, very similar in both shape and position to the B-form DNA spectrum of the non-specific NFIII oligonucleotide and shows a less significant overall increase in molar ellipticity upon formation of the HIV-L oligonucleotide–NF-κB p50 complex (Fig. 5E). The near UV CD spectrum of the non-specific NFIII oligonucleotide is typical of that of B-form

DNA and the spectrum is unchanged upon formation of the complex between p50 and the non-specific DNA (Fig. 5F).

The far UV CD spectra of p65 homodimer in the absence and presence of specific and non-specific binding site DNA are shown in Figure 6A–C. As with the p50 homodimer spectra, the p65 homodimer signals are relatively small, but application of the CONTIN procedure to the far UV CD p65 homodimer spectra in the absence and presence of DNA over the range 200–240 nm indicates secondary structure contents quite similar to those of p50. Again, while it is possible to state that binding of DNA to p65 homodimers leads to a conformational change in the protein, it is not possible to express this in terms of specific secondary structure changes.

The ability of p65 homodimers to induce structural changes in bound DNA was determined by examination of the near UV region of the CD spectrum. Again, the unusual structure of the H2TF1 oligonucleotide is apparent, with a significant increase in the molar ellipticity maximum amplitude, a change in the position of that maximum in the spectrum and a change in the shape of the H2TF1 CD spectrum upon formation of the complex with p65 (Fig. 6D). Likewise, the B-form DNA-like conformation of the HIV-L κB motif oligonucleotide showed an increase in near UV CD spectrum amplitude, but no change in shape upon formation of specific p65–HIV-L κB motif oligonucleotide complexes (Fig. 6E). The near UV CD spectrum of the non-specific NFIII oligonucleotide showed no change in its B-form DNA-like pattern upon formation of non-specific complexes with p65 (Fig. 6F).

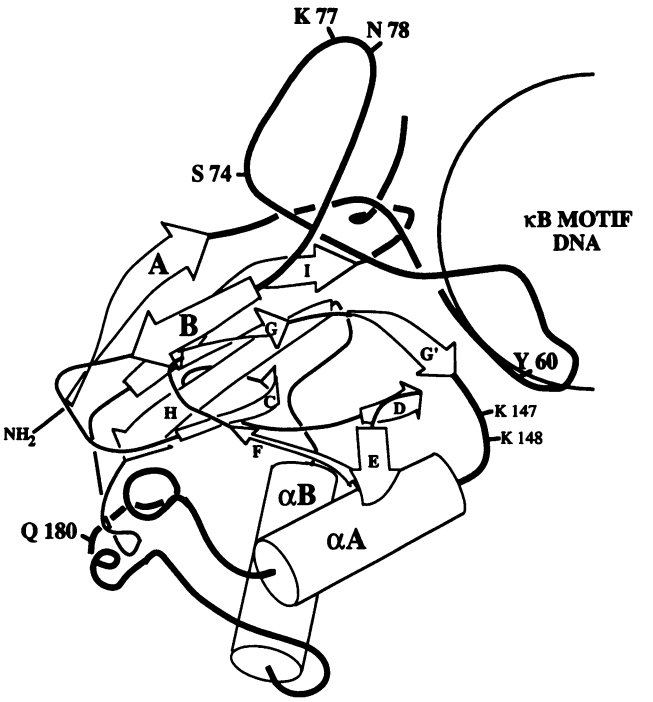

Figure 7. Schematic diagram (adapted from ref 27) of the N-terminal domain of p50 in the specific p50 homodimer–H2TF1 κB motif complex, viewed from along the axis of the κB motif DNA. Those regions of the p50 N-terminal domain which are involved in contacting the κB motif DNA and/or whose proteolytic sensitivity changes in the p50–H2TF1 κB motif complex are indicated in bold, as are the specific amino acid residues whose proteolytic sensitivity changes in the high affinity complex (the data for p50 residue K77 is taken from ref 25). The p50 K147 and K148 residues which are involved in forming hydrogen bonds with backbone phosphates from the minor groove side of the κB motif are also indicated.

DISCUSSION

Conformational changes occurring in both NF-κB proteins and κB motif DNA upon formation of specific NF-κB–κB motif complexes have been demonstrated by proteolytic sensitivity studies and CD spectroscopy. The locations of regions of p50 undergoing conformational changes upon formation of complexes with the high affinity H2TF1 type of κB motif are given schematically in Figure 7. Regions of the p50 N-terminal domain involved in contacting κB motif DNA and/or whose proteolytic sensitivity changes in the DNA–protein complex are indicated in bold. Specific amino acid residues whose proteolytic sensitivity changes in the DNA–protein complex are also indicated in bold. DNA sequence-dependent conformational changes occur both in the p50 N-terminal domain AB loop region and in the (mainly α-helical) region between p50 N-terminal domain β-strands G′ and H. CD spectroscopy reveals that these conformational changes in p50 are reciprocated by structural changes in the H2TF1 κB motif DNA that accompany complex formation. In its unbound form H2TF1 κB motif DNA has an atypical structure which appears to deviate from that of classical B-form DNA.

The X-ray crystallographic structure of the p50 homodimer complexed with an 11 bp $H2K^b$ H2TF1 κB motif with a central A·A mismatch demonstrated that this DNA sequence has several unusual structural features (27). For example, this sequence has an overall twist of 10.7 bp/turn, with a very deep major groove and with a narrow minor groove across the dyad. Further, the DNA axis in the co-crystal was bent towards the p50 dimerization domains by 15° at the junction between the central AAT sequence and the GGGG flanking half-sites, with the GGGG segments having an unusual conformation, similar to the enlarged major groove type of DNA conformation (B_{eg}-DNA) which has been identified in several types of DNA–protein complex and which has characteristics of both B- and A-form DNA (27,37). The authors noted that due to the short length of the MHC H2TF1 oligonucleotide it was not possible to make firm conclusions about the actual overall bend or the effects of probable backbone contacts outside the 11 bp H2TF1 κB motif.

The present CD spectroscopy study shows that conformational changes occur in κB motif DNA upon binding NF-κB proteins, most dramatically in the case of the H2TF1 κB motif. Although the precise conformation of the free H2TF1 κB motif oligonucleotide is uncertain, the increase in its molar ellipticity in the protein–DNA complex, most likely resulting from an increase in base stacking, probably reflects an unwinding of the H2TF1 duplex in the protein–DNA complex. Similarly, the non-B-form DNA CD spectrum of the H2TF1 κB motif oligonucleotide reveals that this DNA sequence has an inherently unusual conformation.

In contrast, the p50–κB motif X-ray crystallographic structure published simultaneously by Ghosh and co-workers using the κB motif 5′-(T)GGGAATTCCC-3′ suggested that, other than a slight bend at the centre of the κB motif and a slight unwinding (with about 11 bp/turn) of the duplex, the DNA structure did not deviate significantly from that of B-form DNA (28). The apparent contradiction between these two crystallographic structures was suggested to result from slightly different orientations of the

N-terminal domains in the complex with the H2TF1 motif, allowing similar specific contacts to be made closer to the dyad axis (27). As further contacts between p50 and the backbone of the DNA are possible in complexes involving longer DNA segments (27), it is conceivable that greater conformational changes may occur in the protein when p50 is complexed to the H2TF1 κB motif in the context of a longer oligonucleotide. However, such conformational changes do not seem to lead to gross bending of κB motif DNA by purified p50 homodimers, as measured by several independent assays using HIV and MHC (H2TF1) κB motifs (38). It does seem likely, however, from the increased molar ellipticity seen for both the H2TF1 and HIV-L κB motif oligonucleotides after forming protein–DNA complexes with p50 and p65 homodimers that a slight unwinding of the κB motif duplex is a general phenomenon upon protein–DNA complex formation.

The present observations of DNA sequence-dependent protection from proteinase digestion of p50 homodimers at residues Y60, S74 and N78 provide evidence for a model invoking conformational changes in the p50 N-terminal domain AB loop upon binding to high affinity DNA sites such as the H2TF1 κB motif. As the Y60 residue is in intimate contact with the κB motif DNA (27,28) (Fig. 7), the observed differences in chymotrypsin sensitivity might be explained by the higher affinity of p50 homodimers for the H2TF1 κB motif compared with the HIV-L type of κB motif. However, previous studies have shown that cleavage by trypsin at the K77 residue of p50 can be almost totally blocked by forming a complex with the high affinity H2TF1 type of κB motif (25). If those and the present results are correlated with the X-ray crystallographic structures of p50 homodimer–κB motif complexes (27,28) it can be seen that the p50 AB loop S74, K77 and N78 residues are exposed on the surface of p50 and are distant from the AB loop residues involved in contacting the bound κB motif oligonucleotide (Fig. 7), ruling out a simple occlusion effect and supporting a DNA sequence-dependent conformational change in the p50 N-terminal domain AB loop.

It should be noted, however, that Müller and co-workers, in their X-ray crystallographic structure of the p50 homodimer–H2TF1 κB motif complex, suggest that with longer DNA segments the second part of the p50 N-terminal domain AB loop, which contains three lysine residues, may be involved in forming additional contacts with backbone phosphates outside the 11 bp H2TF1 κB site (27). This potential involvement of some or all of p50 AB loop residues K77, K79 and K80, in combination with the more N-terminal residues of the AB loop, in forming a C-shaped clamp across the DNA duplex could provide an explanation for the DNA sequence-dependent proteinase protection of p50 residues S74, K77 and N78 by their involvement in further conformational changes in the AB loop structure.

Similarly, the enhanced cleavage of p50 at residue Q180 by proteinase K in the presence of the high affinity H2TF1 type of κB motif oligonucleotide suggests that a conformational change occurs in the mainly α-helical insertion between p50 N-terminal domain β-strands G′ and H when p50 is complexed with the H2TF1 oligonucleotide. As p50 lysine residues 147 and 148 are involved in forming hydrogen bonds with backbone phosphates from the minor groove side of the κB motif (27,28; Fig. 7), it seems possible that this hydrogen bonding interaction causes a conformational change in this region of p50. A conformational change in this loop region could be transmitted via the rigid αA α-helix and subsequently be reflected in the DNA sequence-dependent enhanced proteinase K sensitivity of p50 residue Q180 (Fig. 7).

Although changes in the far UV CD spectrum of p50 homodimers are detected upon formation of either specific or non-specific protein–DNA complexes, these changes may not represent the sequence-dependent conformational changes seen in the p50 N-terminal domain AB loop region and in the mainly α-helical insertion between β-strands G′ and H. Rather, these conformational changes induced upon binding any DNA sequence might represent a packing down at the interface between the N-terminal and C-terminal domains, it having been proposed that in the absence of DNA the two domains may be fairly loosely tethered (27). Alternatively, the conformational changes induced in the p50 homodimer upon binding any DNA might reflect some global change in the structure of one or other domain, such as a transition from a molten globular state to a more rigid structure. Such a transition might explain the complete degradation of p50 homodimers in the absence of DNA upon trypsin digestion versus protection in the presence of the H2TF1 κB motif oligonucleotide (25). A similar transition from a metastable molten globular state to a more rigid tertiary structure has been observed in a cytosine (C5)-specific DNA methyltransferase DNA recognition subunit upon binding DNA (39).

Changes in protein and binding site DNA conformation upon complex formation are likely to be very common. For example, binding of the yeast GCN-4 protein basic region–leucine zipper (bZIP) peptide homodimer to specific AP-1 or ATF/CREB DNA sites induces small changes in the oligonucleotide conformation. Whereas large changes in the GCN-4 conformation (corresponding to induction of α-helical structure in the basic region of the peptide) occur upon formation of the specific DNA–protein complex, but not upon formation of a non-specific complex (40). Similar increases in the α-helical content of Fos and Jun bZIP proteins were seen upon formation of complexes with a specific AP-1 oligonucleotide, but not with a non-specific oligonucleotide (41).

ACKNOWLEDGEMENTS

We are most grateful to Dr Graham Kemp and Paul Talbot for N-terminal protein sequencing and Bill Blyth for photographic services. This work was supported by the BBSRC and the European Communities concerted action project ROCIO.

REFERENCES

1 Nolan,G.P. and Baltimore,D. (1992) *Curr. Opin. Genet. Dev.*, **2**, 211–220.
2 Kieran,M., Blank,V., Logeat,F., Vandekerckhove,J., Lottspeich,F., LeBail,O., Urban,M.B., Kourilsky,P., Baeuerle,P.A. and Israël,A. (1990) *Cell*, **62**, 1007–1018.
3 Ghosh,S., Gifford,A.M., Riviere,L.R., Tempst,P., Nolan,G.P. and Baltimore,D. (1990) *Cell*, **62**, 1019–1029.
4 Schmid,R.M., Perkins,N.D., Duckett,C.S., Andrews,P.C. and Nabel,G.J. (1991) *Nature*, **352**, 733–736.
5 Bours,V., Burd,P.R., Brown,K., Villalobos,J., Park,S., Ryseck,R.-P., Bravo,R., Kelly,K. and Siebenlist,U. (1992) *Mol. Cell. Biol.*, **12**, 685–695.
6 Nolan,G.P., Ghosh,S., Liou,H.-C., Tempst,P. and Baltimore,D. (1991) *Cell*, **64**, 961–969.
7 Ruben,S.M., Dillon,P.J., Schreck,R., Henkel,T., Chen,C.-H., Maher,M., Baeuerle,P.A. and Rosen,C.A. (1991) *Science*, **251**, 1490–1493.
8 Ryseck,R.-P., Bull,P., Takamiya,M., Bours,V., Siebenlist,U., Dobrzanski,P. and Bravo,R. (1992) *Mol. Cell. Biol.*, **12**, 674–684.
9 Ruben,S.M., Klement,J.F., Coleman,T.A., Maher,M., Chen,C.-H. and Rosen,C.A. (1992) *Genes Dev.*, **6**, 745–760.
10 Brownell,E., Mittereder,N. and Rice,N.R. (1989) *Oncogene*, **4**, 935–942.

11 Wilhelmsen,K.C., Eggleton,K. and Temin,H.M. (1984) *J. Virol.*, **52**, 172–182.
12 Steward,R. (1987) *Science*, **238**, 692–694.
13 Ip,Y.T., Reach,M., Engstrom,Y., Kadalayil,L., Cai,H., Gonzalez-Crespo,S., Tatei,K. and Levine,M. (1993) *Cell*, **75**, 753–763.
14 Grimm,S. and Baeuerle,P.A. (1993) *Biochem. J.*, **290**, 297–308.
15 Baeuerle,P.A. and Baltimore,D. (1989) *Genes Dev.*, **3**, 1689–1698.
16 Sen,R. and Baltimore,D. (1986) *Cell*, **46**, 705–716.
17 Coleman,T.A., Kunsch,C., Maher,M., Ruben,S.M. and Rosen,C.A. (1993) *Mol. Cell. Biol.*, **13**, 3850–3859.
18 Matthews,J.R., Kaszubska,W., Turcatti,G., Wells,T.N.C. and Hay,R.T. (1993) *Nucleic Acids Res.*, **21**, 1727–1734.
19 Toledano,M.B., Ghosh,D., Trinh,F. and Leonard,W.J. (1993) *Mol. Cell. Biol.*, **13**, 852–860.
20 Liu,J., Sodeoka,M., Lane,W.S. and Verdine,G.L. (1994) *Proc. Natl. Acad. Sci. USA*, **91**, 908–912.
21 Toledano,M.B. and Leonard,W.J. (1991) *Proc. Natl. Acad. Sci. USA*, **88**, 4328–4332.
22 Kumar,S., Rabson,A.B. and Gélinas,C. (1992) *Mol. Cell. Biol.*, **12**, 3094–3106.
23 Matthews,J.R., Wakasugi,N., Virelizier,J.-L., Yodoi,J. and Hay,R.T. (1992) *Nucleic Acids Res.*, **20**, 3821–3830.
24 Hayashi,T., Ueno,Y. and Okamoto,T. (1993) *J. Biol. Chem.*, **268**, 11380–11388.
25 Hay,R.T. and Nicholson,J. (1993) *Nucleic Acids Res.*, **21**, 4592–4598.
26 Fujita,T., Nolan,G.P., Ghosh,S. and Baltimore,D. (1992) *Genes Dev.*, **6**, 775–787.
27 Müller,C.W., Rey,F.A., Sodeoka,M., Verdine,G.L. and Harrison,S.C. (1995) *Nature*, **373**, 311–317.
28 Ghosh,G., Van Duyne,G., Ghosh,S. and Sigler,P.B. (1995) *Nature*, **373**, 303–310.
29 Clark,L., Nicholson,J. and Hay,R.T. (1989) *J. Mol. Biol.*, **206**, 615–626.
30 Clark,L. and Hay,R.T. (1989) *Nucleic Acids Res.*, **17**, 499–516.
31 Clark,L., Matthews,J.R. and Hay,R.T. (1990) *J. Virol.*, **64**, 1335–1344.
32 Urban,M.B., Schreck,R. and Baeuerle,P.A. (1991) *EMBO J.*, **10**, 1817–1825.
33 Zabel,U., Schreck,R. and Baeuerle,P.A. (1991) *J. Biol. Chem.*, **266**, 252–260.
34 Laemmli,U.K. (1970) *Nature*, **227**, 680–685.
35 Matthews,J.R., Watson,E., Buckley,S. and Hay,R.T. (1993) *Nucleic Acids Res.*, **21**, 4516–4523.
36 Provencher,S.W. and Glöckner,J. (1981) *Biochemistry*, **20**, 33–37.
37 Nekludova,L. and Pabo,C.O. (1994) *Proc. Natl. Acad. Sci. USA*, **91**, 6948–6952.
38 Kuprash,D.V., Rice,N.R. and Nedospasov,S.A. (1995) *Nucleic Acids Res.*, **23**, 427–433.
39 Hornby,D.P., Whitmarsh,A., Pinarbasi,H., Kelly,S.M., Price,N.C., Shore,P., Baldwin,G.S. and Waltho,J. (1994) *FEBS Lett.*, **355**, 57–60.
40 Weiss,M.A., Ellenberger,T., Wobbe,C.R., Lee,J.P., Harrison,S.C. and Struhl,K. (1990) *Nature*, **347**, 575–578.
41 Patel,L., Abate,C. and Curran,T. (1990) *Nature*, **347**, 572–575.